AD-A083 382 AIR FORCE AVIONICS LAB WRIGHT-PATTERSON AFB OH F/G 9/5
THE APPLICATION OF INTEGRATED OPTICS TO COMPUTING.(U)
JAN 80 D A WILLE
UNCLASSIFIED AFAL-TR-79-1196 NL

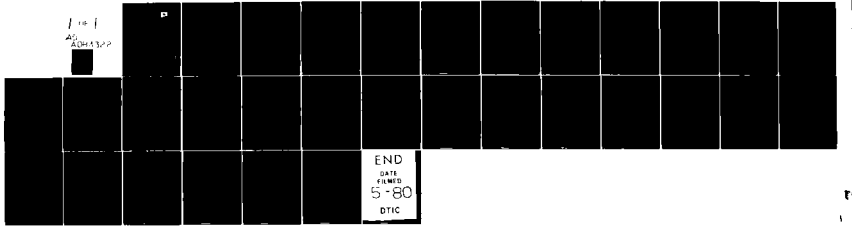

END
DATE FILMED
5-80
DTIC

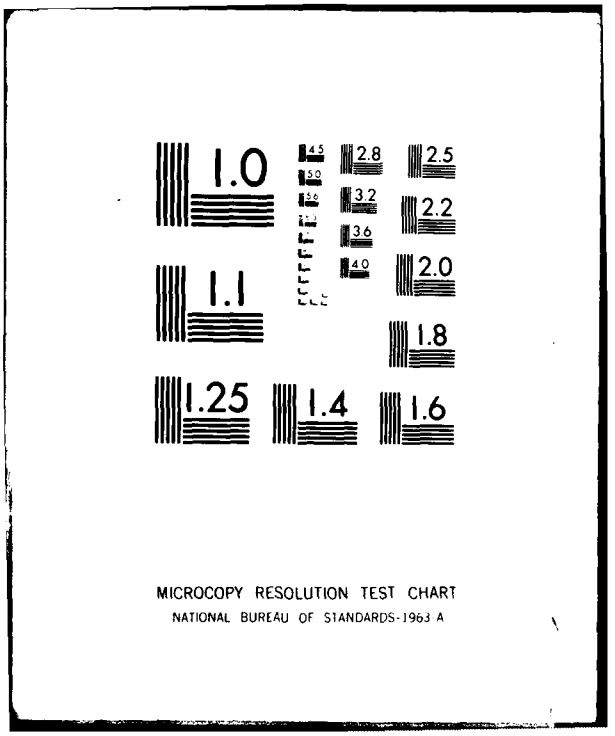
1.0
1.1
1.25
1.4
1.6
1.8
2.0
2.2
2.5
2.8
3.2
3.6
4.0
4.5
5.0
5.6
MICROCOPY RESOLUTION TEST CHART
NATIONAL BUREAU OF STANDARDS-1963 A

AFAL-TR-79-1196

LEVEL II

(2) NW

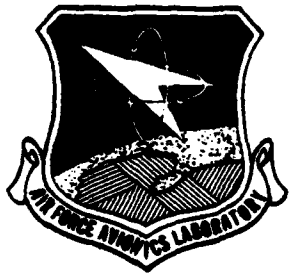

AD A083322

THE APPLICATION OF INTEGRATED OPTICS TO COMPUTING

Douglas A. Wille, PhD
Electro-Optics Technology Branch
Electronic Technology Division

January 1980

TECHNICAL REPORT AFAL-TR-79-1196

Final Report

Approved for public release; distribution unlimited.

AIR FORCE AVIONICS LABORATORY
AIR FORCE WRIGHT AERONAUTICAL LABORATORIES
AIR FORCE SYSTEMS COMMAND
WRIGHT-PATTERSON AIR FORCE BASE, OHIO 45433

NOTICE

When Government drawings, specifications, or other data are used for any purpose other than in connection with a definitely related Government procurement operation, the United States Government thereby incurs no responsibility nor any obligation whatsoever; and the fact that the government may have formulated, furnished, or in any way supplied the said drawings, specifications, or other data, is not to be regarded by implication or otherwise as in any manner licensing the holder or any other person or corporation, or conveying any rights or permission to manufacture, use, or sell any patented invention that may in any way be related thereto.

This report has been reviewed by the Information Office (OI) and is releasable to the National Technical Information Service (NTIS). At NTIS, it will be available to the general public, including foreign nations.

This technical report has been reviewed and is approved for publication.

Douglas A. Wille

DOUGLAS A. WILLE, Physicist
Electro-Optics Techniques and
Applications Group
Electro-Optics Technology Branch

Kenneth R. Hutchinson

KENNETH R. HUTCHINSON, Chief
Electro-Optics Techniques and
Applications Group
Electro-Optics Technology Branch

FOR THE COMMANDER

Ronald F. Paulson

RONALD F. PAULSON, Chief
Electro-Optics Technology Branch
Electronic Technology Division

"If your address has changed, if you wish to be removed from our mailing list, or if the addressee is no longer employed by your organization please notify AFAL/DHO-2 ,W-PAFB, OH 45433 to help us maintain a current mailing list".

Copies of this report should not be returned unless return is required by security considerations, contractual obligations, or notice on a specific document.

SECURITY CLASSIFICATION OF THIS PAGE (When Data Entered)

REPORT DOCUMENTATION PAGE

READ INSTRUCTIONS BEFORE COMPLETING FORM

1. REPORT NUMBER: AFAL-TR-79-1196	2. GOVT ACCESSION NO.: AD-A083 322
3. RECIPIENT'S CATALOG NUMBER:	
4. TITLE (and Subtitle): THE APPLICATION OF INTEGRATED OPTICS TO COMPUTING.	5. TYPE OF REPORT & PERIOD COVERED: Final Report
	6. PERFORMING ORG. REPORT NUMBER:
7. AUTHOR(s): Dr. Douglas A. Wille, PhD	8. CONTRACT OR GRANT NUMBER(s):
9. PERFORMING ORGANIZATION NAME AND ADDRESS: Air Force Avionics Laboratory (DHO-2) AF Wright Aeronautical Laboratories Wright-Patterson Air Force Base, Ohio 45433	10. PROGRAM ELEMENT, PROJECT, TASK AREA & WORK UNIT NUMBERS: 62204F 20010222
11. CONTROLLING OFFICE NAME AND ADDRESS: Air Force Avionics Laboratory (AFAL/DH) AF Wright Aeronautical Laboratories Wright-Patterson Air Force Base, Ohio 45433	12. REPORT DATE: January 1980 13. NUMBER OF PAGES: 32
14. MONITORING AGENCY NAME & ADDRESS (if different from Controlling Office): 34	15. SECURITY CLASS. (of this report): UNCLASSIFIED 15a. DECLASSIFICATION/DOWNGRADING SCHEDULE:

16. DISTRIBUTION STATEMENT (of this Report)

Approved for public release; distribution unlimited.

17. DISTRIBUTION STATEMENT (of the abstract entered in Block 20, if different from Report)

18. SUPPLEMENTARY NOTES

19. KEY WORDS (Continue on reverse side if necessary and identify by block number)

Bistable optical devices
Residue arithmetic
Optical computing
Integrated optics

20. ABSTRACT (Continue on reverse side if necessary and identify by block number)

Recent developments in bistable optical devices and residue arithmetic processing have shown there is a significant potential application of optics to computing. The ability to perform these functions using integrated optics provides the capability for providing a high device density and enhances the application to computing. An introduction to bistable optical devices and residue arithmetic is provided and the fundamental limit to optical computing set by thermal problems is addressed. It is concluded that the limits previously proposed are not applicable and thermal loss can potentially be very low.

DD FORM 1 JAN 73 1473 EDITION OF 1 NOV 65 IS OBSOLETE

SECURITY CLASSIFICATION OF THIS PAGE (When Data Entered)

011 670

TABLE OF CONTENTS

LIST OF ILLUSTRATIONS

SECTION I

INTRODUCTION

Integrated optics offers the advantage of performing optical functions within a very small physical package. Implicit in this small size is the potential for integrating a large number of elements onto a single substrate, the limit on packing density being the limits of photolithography. Recent developments in the areas of bistable optical devices and residue arithmetic have shown there is a significant potential for performing computational functions with optical devices. Implementing the concepts with integrated optics technology then can produce a capability to perform computations with the inherent speed advantage of optics.

First, consider the bistable optical device. It becomes apparent from a brief study of bistable optical devices that a prominent application is to perform logic functions. Since this application is so prominent, it is natural to consider the idea of an optical computer. The possibility of an optical computer has been considered in the past and the conclusion was reached that thermal dissipation problems will prevent a sufficiently dense packing of devices to use the high speed potential of optics. The basic assumption is that energy in the signal used to switch a gate must be dissipated at or near the gate as occurs with electronic functions. Analysis then shows that the theoretical limit for electronic devices is significantly lower than for optical devices. These analyses were performed without a knowledge of bistable optical devices and are in error in terms of the basic assumption.

While it cannot be demonstrated that an optical computer is feasible, it is at least conceivable and one can consider data processing in a computer format with no RC time constant limitations. To some extent, the point is moot since the limitations ascribed to optics apply to a large scale computer such as the IBM 360. The Air Force has no specific need to develop such computers, but there is a need for on-board computational capabilities in aircraft. Without an a priori ban on optics such applications can be considered as important uses for bistable optical devices.

The area of residue arithmetic is interesting since it shows a way of performing computations that are many times faster than can be done with binary arithmetic. A review of residue arithmetic operations shows that the basic functions can be performed optically in an integrated optics format.

Both the bistable device area and the residue arithmetic area are applicable to optical computing and represent a significant application potential for integrated optics.

In the following discussion a brief overview of bistable optical devices and residue arithmetic is provided. A discussion of the theoretical limits of power dissipation is also provided.

SECTION II

BISTABLE OPTICAL DEVICES

The possibility of a bistable optical device was first suggested in 1969 (Reference 1) but it wasn't until 1976 (Reference 2) that such a device was first demonstrated. The first demonstration used sodium vapor in a Fabry-Perot interferometer. Operation depended on the nonlinear dispersion of the sodium vapor near the absorption lines. Since then a Fabry-Perot with a Kerr effect medium (MBRA) (Reference 3) has been demonstrated, as have a number of hybrid devices using electrical feedback (References 4, 5, and 6) including integrated optics format (Reference 7).

For discussion purposes the simplest system to examine is a hybrid Fabry-Perot device using a linear electro-optic material as shown in Figure 1. The Fabry-Perot is initially adjusted so the Fabry-Perot is not tuned to its high transmission state. The output power is sampled using a beam splitter, detected and then amplified. The amplified signal appears as a voltage across the linear electro-optic material and produces a phase shift in the crystal, moving the operating point nearer to a

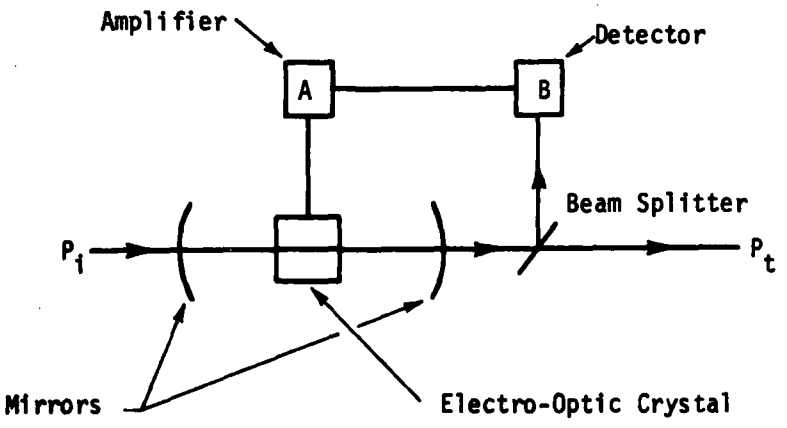

Figure 1. Hybrid Fabry-Perot BOD

tuning peak of the Fabry-Perot. The material is linear, but since the voltage is proportional to the output intensity, and thus E^2, we effectively have a nonlinear feedback. The transmission of a Fabry-Perot can be written as:

$$\tau = \frac{P_t}{P_i} = \frac{(1 - R)^2}{(1 - R)^2 + 4R\sin^2\delta}$$

where τ is the transmission, P_i the input power, P_t the output power, R is the Fabry-Perot mirror reflectivity and δ is the one-way phase shift. Taking the feedback into account, we can write the phase shift as:

$$\delta = \frac{2\pi n l}{\lambda} + KP_t$$

where n is the zero voltage index, l is the cavity length, λ is the free space wavelength and K is a constant depending on the detector and amplifier characteristics. Rearranging this last equation we can write:

$$\tau = \frac{P_t}{P_i} = \frac{\delta - 2\pi n l/\lambda}{KP_i}$$

and we thus have a pair of simultaneous equations. P_t is not readily written in terms of P_i, and we need to resort to either a graphical solution as shown in Figure 2 or a computer solution. Using the computer to solve the equations numerically is implemented as follows. If we can substitute the last equation in the first, we can write:

$$P_i = P_t\,[1 + A\sin^2 2\pi(aP_t + b)]$$

where $A = 4R/(1 - R)^2$, $K = 2\pi a$, $b = nl/\lambda$. Thus, for a given P_t we can calculate the value of P_i for a given selection of b. Since we have the variables P_i, P_t and b the solution is a surface-in-three space that has a very interesting fold as shown in Figure 3. I have shown only one fold, but in fact there are an infinite number of folds that require large input powers to be attainable and, thus, may not be of practical interest. To see the bistable characteristic we note that for a given

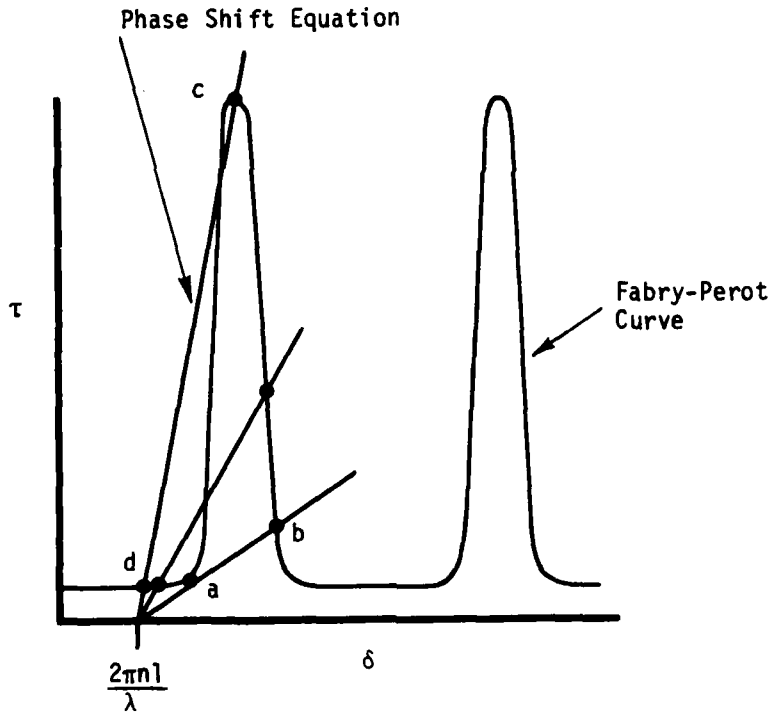

Figure 2. Graphical Solution

The dots represent operating points. The outer straight lines represent the critical switching points and the middle represents the bistable operation. The labelled points correspond to Figure 4.

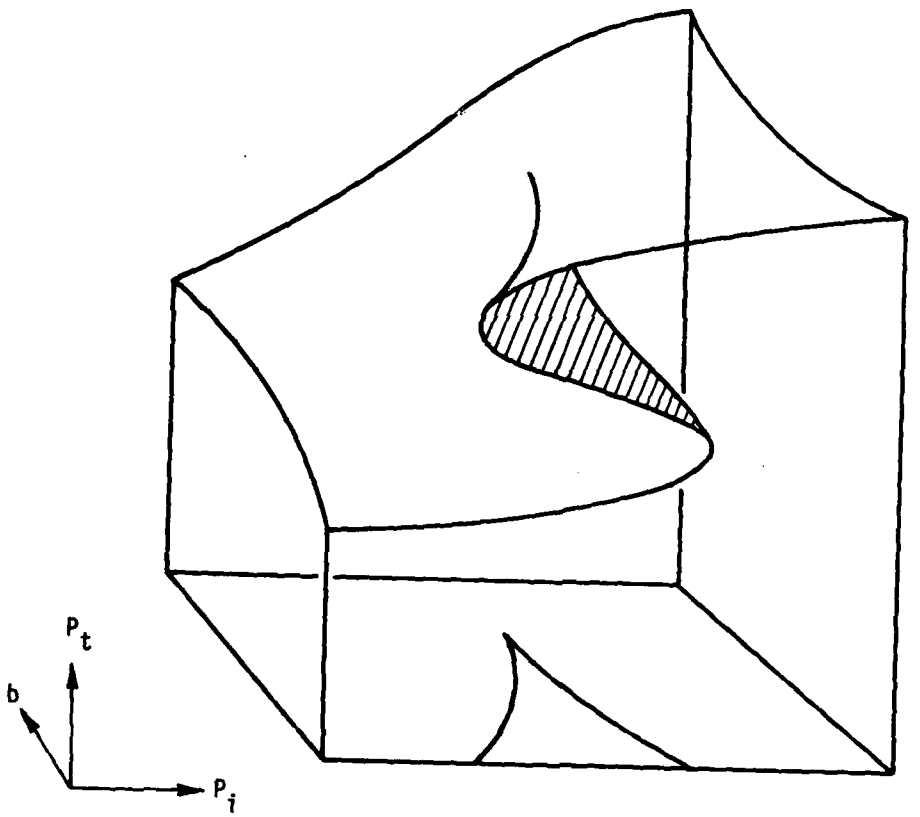

Figure 3. Bistable Surface

value of b, which represents the mistuning of the Fabry-Perot, we get a curve as shown in Figure 4. If the input power is increased from zero, P_t increases slowly until the point a is reached where the slope becomes infinite and the output power increases suddenly to point b. As P_i is increased beyond b there is only a small increase in P_t. Then consider lowering P_i. As P_i proceeds below b, there is only a small decrease in P_t until point c is reached where the slope again goes to infinity and the system jumps to point d. Thus, we have traced out a hysteresis loop between two stable output states.

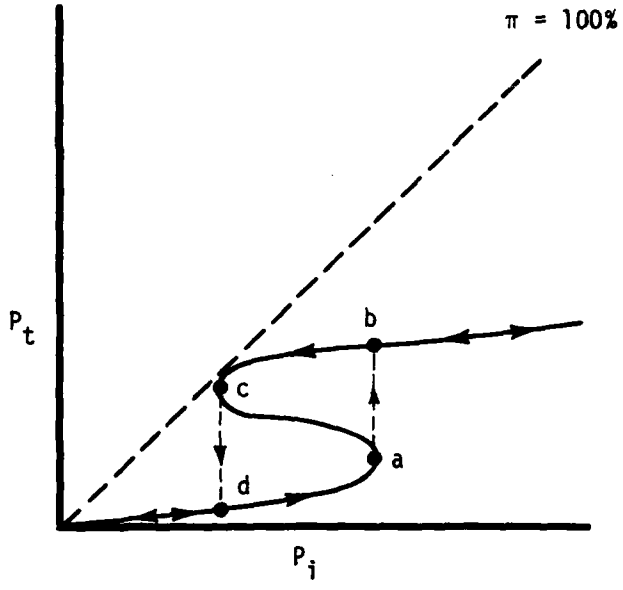

Figure 4. Hysteresis Curve

To consider the applications, I have shown in Figure 5 a series of P_t vs P_i curves for increasing values of b. In the upper graph the first fold is too far away to be reached by reasonable input powers. As we proceed, the fold "comes into view" and then reaches a low power "S" shaped region, which is the center graph. In this case, the device has application both as a memory element and as a switch. As a memory element, we can consider the upper and lower levels as 1 and 0 respectively. As a switch, we can see that a control beam of power greater than that at a (Figure 4) will turn the device "on" and by lowering the input power below that at d, we can turn the device "off". It is assumed here that the "on" and "off" states would be explored by a second beam of small enough intensity to not alter the state.

Operation for logic gates can best be obtained with the b value in the fourth curve. Referring to Figure 6(a) the amplitude of two concurrent optical pulses is shown where either pulse is large enough to turn the device on and we have an "or" gate. In Figure 6(b) we have the case where neither pulse is large enough to turn the device on and both pulses must be present for an on state, thus giving an "and" gate.

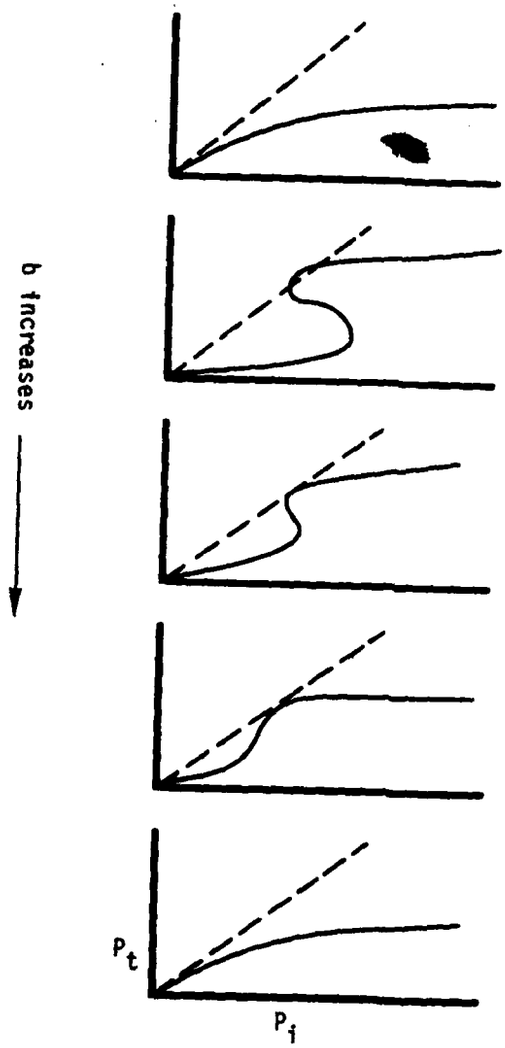

Figure 5. Effects of Variation of b

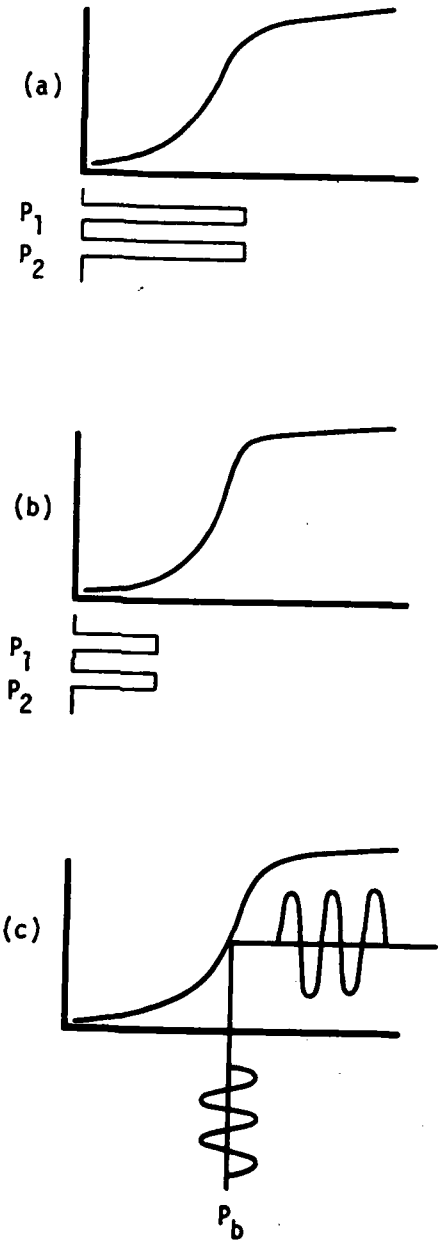

Figure 6. Bistable Application

In this state, we also have limiter action since increasing the input intensity beyond the "on" power produces very little change in the output power. The Fabry-Perot type device is basically a three-port device, and the input power that is not transmitted appears as a reflected power and constitutes a third port. Since it is the inverse of the transmission it provides a negation function and we have "nor" and "nand" gate capabilities. In this same mode, we can also show amplifier action as shown in Figure 6(c). If an input power P_b provides a bias as shown, a variation of the input power about, the bias level will be amplified as shown.

Another interesting implementation is shown in Figure 7A. In this case, we have so called $\Delta\beta$ reversal switch (Reference 6) between two waveguides. The feedback from the sampled beam is used to switch the output from the lower channel waveguide (zero input power condition) to the upper channel waveguide. We consider an input beam made up of pulses as shown in Figure 7B. In the Figure, P_c is the power required for the high output condition in terms of an "S" curve (port 1) and P_a is the power for the low output condition (port 2). In the portion of the input (Reference 1), the input power is lowered below P_a to reset the device and then in region (Reference 2) the power returns either to the operating level or becomes higher than P_c and, thus either port 1 or port 2 is selected. A bit stream of the indicated intensity follows the two initial addressing pulses. This is a very clear example of a case where the power used for switching the device is part of the optical stream and is not dissipated at the gate.

Note that the system described was outlined in terms of a specific device, but the characteristics apply to any bistable device whether purely optical or hybrid. Also note that the system is a perfect example of the cusp catastrophe described in catastrophe theory (Reference 8) and the cusp is evident in the trace of the fold edges on the $b - P_i$ plane in Figure 3.

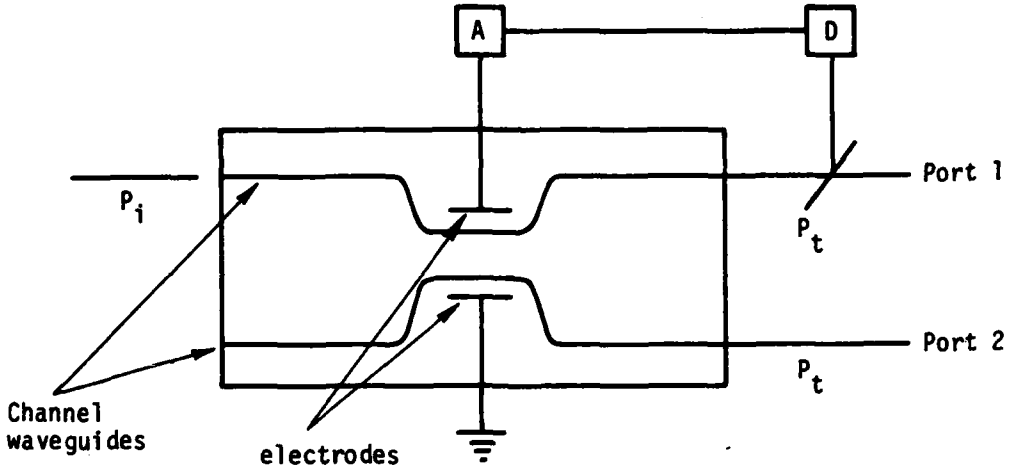

Figure 7A. $\Delta\beta$ Switch with Feedback

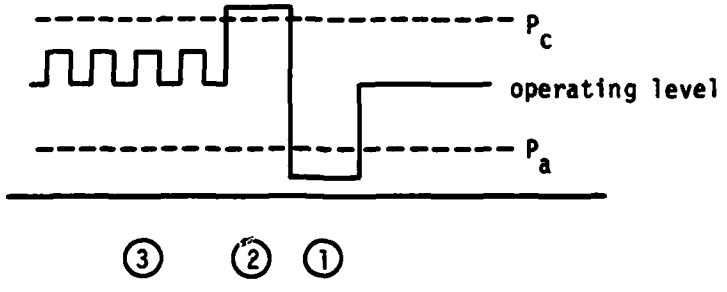

Figure 7B. Self-Addressed Data Stream

Bistability has been shown in a number of implementations, which are described briefly below, preceded by the references.

(Reference 2) The device demonstrated uas a Fabry-Perot interferometer filled with Na vapor and the effect used was the nonlinear dispersion near the Na absorption lines. A 12 mW dye laser was used to show bistability but no risetimes were quoted.

(Reference 9) A Fabry-Perot with an enclosed ruby rod was used and operation depended on nonlinear dispersion. The source was a ruby laser with a 20 mW average output. The laser was Q-switched and, thus, had a high output power. Again, no risetime numbers were given.

(Reference 4) This is a hybrid device which is shown above in Figure 1. The material was KDP. Switching was accomplished with 1 mW but no risetimes are given.

(Reference 3) This device is a Fabry-Perot using MBBA as a Kerr liquid. Switch times were in the μsec range and were dominated by the MBBA relaxation times. A Q-switched ruby laser was the source.

(Reference 7) This is a hybrid device using a Fabry-Perot built onto a diffused waveguide in $LiNbO_3$. Hysteresis was observed with a 5 nW input. Switching time was 200 μsec with 1 pJ switch energy. A hybrid device is projected with no amplification that can provide 1 nsec switch time, 1 pJ switch energy at 1 mW power level.

(Reference 5) This is a hybrid device using bulk $LiNbO_3$ in a standard polarization rotation modulator format. Switching was accomplished with a .5 mW HeNe laser.

(Reference 6) This is the hybrid device shown in Figure 7. The hysteresis curve was obtained by operating between 10 and 70 nW. The switch time was 300 μsec and the switch energy was 3 pJ.

The implementations listed above are only a sample of what has appeared in the literature, but are representative. The hybrid devices are interesting demonstrations but are not likely to be useful in competing

with electronic circuitry since they themselves require electrical connections for operation and would be subject to the same risetime limitations. The completely optical devices that have been demonstrated are bulk devices and require relatively large optical powers for operation. The requirement for a useful device is an all optical device that can be made in an integrated optics format and does not require large optical power for operation. Such devices are feasible and can be expected to be demonstrated in the near future.

SECTION III

RESIDUE ARITHMETIC

An interesting application of integrated optics arises in the use of residue arithmetic to perform computer functions instead of the usual binary arithmetic and has been proposed in the literature (Reference 10).

To understand the application, we need a small digression into the results of modern algebra (Reference 11). The first basic point is expressed as follows:

Euclidean Algorithm

For any integers a, b we find integers p, q such that

$$a = qb + r$$

where q is the quotient and r is the remainder. We then introduce the concept of congruence, which has the sumbol $\equiv$.

Congruence

Given m, for any two integers a, b we can write, by the Euclidean algorithm,

$$a = q_a m + r_a$$

$$b = q_b m + r_b$$

Then $a \equiv b \pmod{m}$

if and only if $r_a = r_b$.

Thus, we say a is congruent to b modulo m if the remainder for a equals the remainder for b. To say it another way, two integers are congruent relative to a modulus m if they differ by a multiple of m. A familiar example of congruence is given by ordinary clock time. Thus we speak 2 o'clock and not 14 o'clock.

Thus, given any modulus m we can reduce all the integers into congruence classes mod m. Let us then suppose that we have a set of moduli $m_1, m_2, \ldots m_n$ such that all the moduli are relatively prime. If for an integer a we find its remainder, or residue, for each modulus, we can represent a as an n-tuple by

$$a = (r_1, r_2, \ldots, r_n)$$

which is essentially the same as representing a vector as an n-tuple of its components. Moreover, it can be easily shown that this representation is unique for any a such that

$$a \leq \prod_{i=1}^{n} m_i - 1$$

To see the advantage of residue arithmetic over binary arithmetic, we will compare some simple operations in each system. In performing addition in a binary form the basic function can be shown in terms of the diagrams in Figure 8. The basic procedure for adding 2 single digit binary numbers utilizes the half adder. The two inputs A, B can be 0 or 1 and the outputs are the sum and the carry digit (i.e., 1 + 1 = 0 and carry 1). The gates are labeled with the Boolean operations. If we add 2-digit binary numbers, the right most digits are added by a half adder and the next two digits are added by the full adder, which uses the carry digit as an input. Depending upon the number of digits in the numbers to be added, additional full adders can be included. The significant point here is that binary addition is inherently a serial process. An array of adders would in general be clock driven, but each pair of digits can only be added after sufficient time for the carry digit to be transferred from the proceeding stage. To be specific, consider the addition number 4 and 9. Encoding the numbers we have

$$4 \rightarrow 100$$
$$9 \rightarrow 1001$$

and adding we have

$$\begin{array}{r} 1001 \\ \underline{100} \\ 1101 \end{array}$$

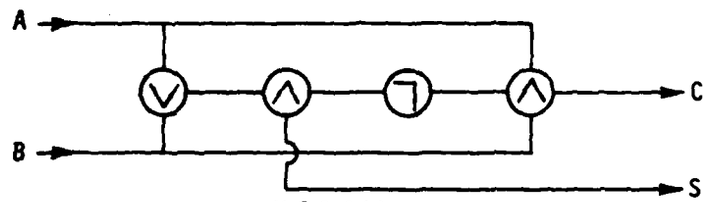

Half Adder

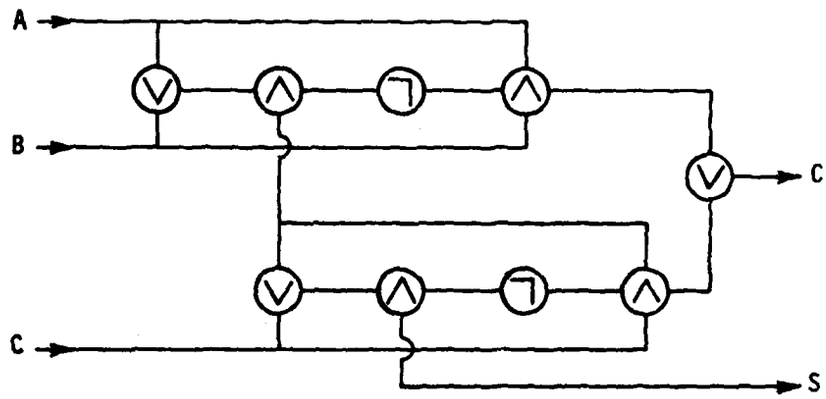

Full Adder

Figure 8. Half and Full Adders

where the serial procedure is quite evident. To do the same operation in residue arithmetic, we use the moduli 2, 3 and 5. Now 4 (mod 2) = 0, 4 (mod 3) = 1, and 4 (mod 5) = 4. The 9 (mod 2) = 1, 9 (mod 3) = 0, 9 (mod 5) = 4. Thus the encoding is

$$4 \rightarrow (0,1,4)$$
$$9 \rightarrow (1,0,4)$$

Adding we have

$$\begin{array}{r} 014 \\ \underline{104} \\ 113 \end{array}$$

where we have used the fact that 8 (mod 5) = 3. We note that 13 (mod 2) = 1, 13 (mod 3) = 1 and 13 (mod 5) = 3 so we indeed have the right answer. The residue numbers can be decoded by algorithm in a way similar to that in which binary numbers are decoded. In adding, each row is added independently since the idea of a carry digit is meaningless here. Thus, all the rows can be added simultaneously and we have the capability for a basically parallel process. The capability to do parallel processing offers a tremendous capacity for increasing the speed of computations. For instance, if a binary number has n digits, the arithmetic processes can be n times faster with residue arithmetic.

To see how integrated optics can apply, consider the simple case of adding the number three to any number mod 5. If the number were 0, 3 + 0 = 3, if it were 1, 3 + 1 = 4, etc. and the addition process becomes a permutation of the integers as shown in Figure 9(A). This sort of operation can be readily implemented in an integrated optics format by using Bragg deflectors as shown in Figure 9(B).

A complete discussion of residue arithmetic has been given by Szabo (Reference 12). An important limitation of residue arithmetic is the fact that division is not always directly realizable because of the integer representation, and is, thus, not likely to be used for general purpose computing. However, there are a number of mathematical operations that do not require division such as fast Fourier transforms and matrix manipulations. Thus, where division is not required and speed is important, residue arithmetic provides an extremely important capability.

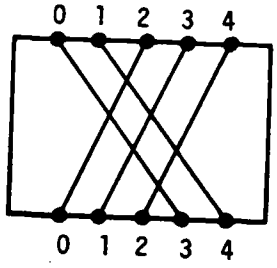

Permutation of Integers Under Addition

A

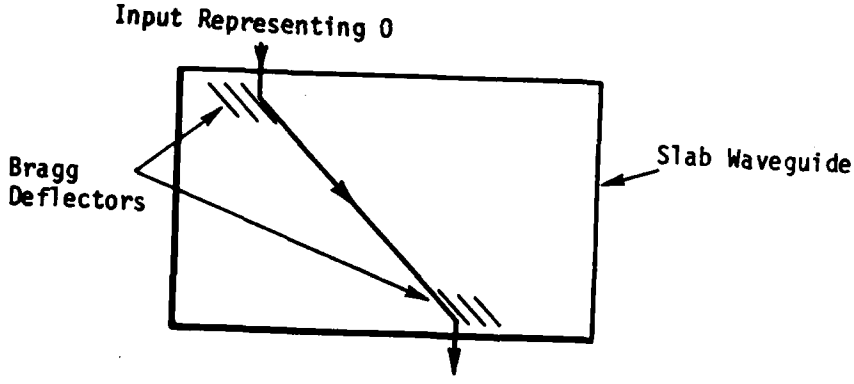

B

Figure 9. Optical Permutation

SECTION IV

OPTICAL LOGIC

The question of whether optical logic could be practically realized has been addressed in the literature. In the latest paper, Keyes (Reference 13) rejects the possibility of optics competing with electronics. Reference is made to an earlier paper as the basic reference (Reference 14). The argument advanced goes as shown below. In electronic logic, the energy used to change the state of the device (i.e., charge transported to produce a voltage) must be dissipated at the device. Fairly good estimates can be made of the maximum rate at which excess power can be removed from a planar array, and thus for a given dissipation a maximum density of devices can be derived. Whatever the intrinsic speed of a device is, if an array of devices requires a wide separation for thermal reasons, then propagation times must be included and the effective speed of the device must be less than the intrinsic speed. Then the assumption is made that for any optical logic device the interaction energy must be dissipated the same way. As the next step, the minimum power required for three different optical techniques is considered. The resultant graph, comparing the electronic and optical theoretic limits, is reproduced in Figure 10. The curves on the graph are as follows: HT, the dotted line, is the thermal transfer limit; COH is based on the phenomena of self-induced transparency; NL is a nonlinear device based on a Pockels effect to produce polarization rotation; BA is a bleachable absorber; CA is a curve I added which is taken from Keyes' 1975 paper (Reference 13) and represents the then commercially available electronics; EL is the fundamental electronics limit where k is the Boltzmann constant, T is the temperature, e is the electronic charge and Z_0 is the impedence of free space. Note that these curves are a lower limit and in practice levels much larger than this must be used both optically and electronically. Thus, for the curve CA the lowest energy per step is $4(10)^{-11}$, which is 10^{10} times the thermal limit of kT.

None of the three optical systems described by Keyes are here considered for optical logic, and the assumption about power loss cannot be evaluated without a specific proposal. Instead we consider the

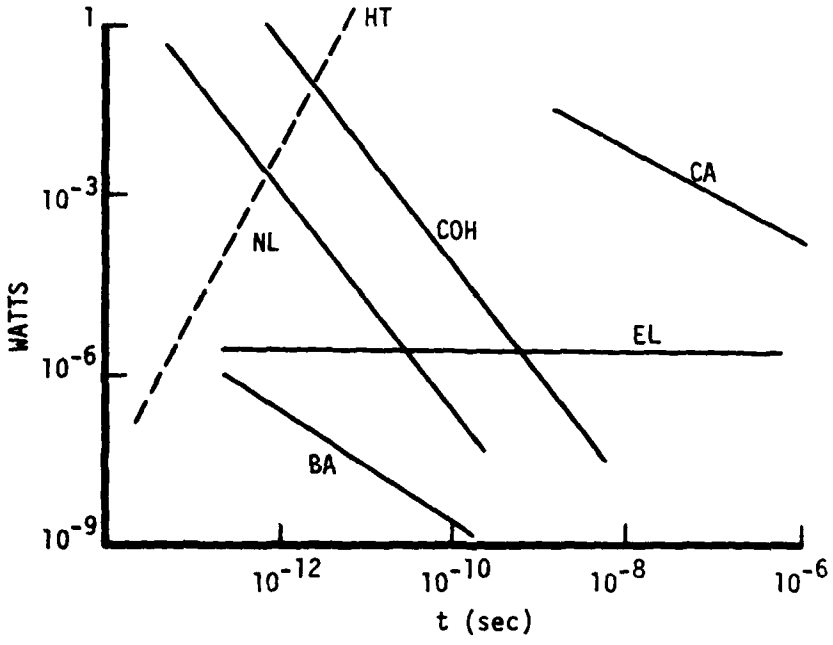

HT	Thermal Transfer Limit
COH	Self-Induced Transparency
NL	Pockels Effect
BA	Bleachable Absorber
CA	Commercially Available Electronics
EL	Electronic Limit $(kT/e)^2/Z_o$

Figure 10. Thermal Limits

bistable optical device, and as a specific example consider a Fabry-Perot device. The Fabry-Perot is basically a three-port device, thus there is an input port defined by the direction of the incident light, an output port defined by the direction of the incident light, an output port defined by the direction of the transmitted light when the device is "on" and an output port defined by the direction of the reflected light when the device is "off." Any light beam incident on the device leaves by one of the output ports. Selection of the output port can be done by the method described for the optical waveguide $\Delta\beta$ reversal switch described above, and the addressing function is part of the data stream. In the and gate function, if one pulse is incident, it exits by way of the reflected port while if two pulses are present they both exit by way of the transmitted port. When the device is in the "on" state, there is a large increase of the optical field intensity in the cavity that builds up with the Fabry-Perot response time. When the incident light is removed the cavity field then decays. One might expect that the decaying field would loose its directional knowledge, since the incident field is gone, and bleed out both output ports, but this is not a loss mechanism.

In examining the above cases, it is seen that there is no inherent loss mechanism involved with the logic function. To find loss mechanisms one must consider the inherent loss in optical propagation. The loss mechanisms fall in the categories of absorption, scattering from non-uniformities or defects in the material and photon-phonon interactions. Both absorption and scattering from defects can, in principle, be reduced to negligible levels. Brillouin scattering, which is due to interactions with thermodynamic fluctuations in material properties and Raman scattering, which is due to interactions with optical phonons are the fundamental loss mechanisms. Brillouin scattering does not, per se, represent a mechanism for heating but the scattered light, which is lost from the waveguide, could be absorbed in the substrate or in nonoptical structures on the substrate. Stokes shifted Raman scattering represents the only fundamental mechanism that can produce heating effects, but the cross section for Raman scattering is typically an order of magnitude

less than that for Brillouin scattering (Reference 15). There is, thus, some suncertainty in fundamental heating effects, the limits being somewhere between Brillouin and Raman scattering.

For practical application, a bistable optical device is required which is all optical and can be fabricated in an integrated optics format. While such a device is, in general, feasible, it has not yet been demonstrated. To make an estimate of potential function, we will consider the all optical Fabry-Perot devices which have been discussed including the ruby rod (Reference 9), the Na-vapor (Reference 2), the MBBA (Reference 3) and the GaAs device (Reference 18). In the GaAs device the nonlinear effect is produced by refractive index changes due to excitonic absorption. It is assumed that an integrated optical device will use a channel waveguide, which we take to have a square cross section. Depending on the materials, the cross sectional dimension can have an order of magnitude ranging from 0.1 μ to 1. μ. The power density required for switching for each of the four devices discussed above is tabulated below. Also tabulated is the laser power required to produce the power density in a 1 μ guide, a .1 μ guide, and the length of the cavity.

	$P_D(w/cm^2)$	$P_o(1\mu)$	$P_o(.1\mu)$	length(cm)
ruby	$1.0(10)^3$	$1.0(10)^{-5}$	$1.0(10)^{-7}$	.5
Na	.5	$5(10)^{-9}$	$5(10)^{-11}$	11
MBBA	$1.7(10)^5$	$1.7(10)^{-3}$	$1.7(10)^{-5}$	1.0
GaAs	$3.4(10)^5$	$3.4(10)^{-3}$	$3.4(10)^{-5}$	$4(10)^{-4}$

The loss data of Miyashita (Reference 16) for optical fibers ranges from 2 db/km at .85 μ down to .2 db/km at 1.55 μ and is approximately at the theoretical limit set by Brillouin scattering. For a given loss, the power goes as

$$P = P_o 10^{-LX/10}$$

where L is the loss in db/km and X is the path length in km. Then

$$dP = -P_o 10^{-LX/10}\left(\frac{L}{10}\ln_e 10\right)dx$$

Thus, in a length dx, the power lost is

$$dP \simeq P_o L(.23)dx$$

and

for dx in cm. $$dP = P_o L(.23)(10)^{-5}dx$$

If we assume a square cross section waveguide of dimension α, the propagating power density P_D is

$$P_D = \frac{P_o}{\alpha^2}$$

For a length dx, the surface area A is

$$A = \alpha dx$$

and the power loss density D_p is

$$D_P = \frac{dP}{dx\alpha} = \frac{P_o L(.23)(10)^{-5}}{\alpha}$$

For a Fabry-Perot with a cavity length dx, the round trip transit time t_r is

$$t_r = \frac{2dx}{c}$$

neglecting the index of the medium in the Fabry-Perot. With a reflectance of .9, the rise time of the cavity, t_{rt}, is approximately

$$t_{rt} \simeq 10\, t_r$$
$$= \frac{20dx}{c}$$
$$= 6.6(10)^{-10}dx$$

Then the energy lost in the rise time, J, is

$$J = t_{rt}\, dP$$

$$= 6.6dx^2 P_o L(.23)(10)^{-5}$$

If there are no material risetime limitations, J represents the minimum energy loss for a switching function.

Tabulated below are the risetime, t_{tr}, the area (αdx) for α=1 and the area for α=.1 for the four materials.

	Risetime	area(α=1)	area(α=.1)
Ruby	$3.3(10)^{-10}$	$5.(10)^{-5}$	$5.(10)^{-6}$
Na	$7.3(10)^{-9}$	$1.1(10)^{-3}$	$1.1(10)^{-4}$
MBBA	$6.6(10)^{-10}$	$1.(10)^{-4}$	$1.0(10)^{-5}$
GaAs	$2.6(10)^{-13}$	$4.(10)^{-8}$	$4.(10)^{-9}$

Tabulated below is the power loss for L=2, .2 and α=1, .1.

Power Loss (dP)

	α=1 L=2	α=1 L=.2	α=.1 L=2	α=.1 L=.2
Ruby	$2.3(10)^{-11}$	$2.3(10)^{-12}$	$2.3(10)^{-13}$	$2.3(10)^{-14}$
Na	$2.5(10)^{-13}$	$2.5(10)^{-14}$	$2.5(10)^{-15}$	$2.5(10)^{-16}$
MBBA	$7.8(10)^{-9}$	$7.8(10)^{-10}$	$7.8(10)^{-11}$	$7.8(10)^{-12}$
GaAs	$5.8(10)^{-12}$	$5.8(10)^{-13}$	$5.8(10)^{-14}$	$5.8(10)^{-15}$

On the basis of the above data, the power loss density is tabulated. This factor represents the thermal loss that must be dissipated by cooling and is in watts/cm^2.

Power Loss Density (w/cm^2)

	α=1 L=2	α=1 L=.2	α=.1 L=2	α=.1 L=.2
Ruby	$4.6(10)^{-7}$	$4.6(10)^{-8}$	$4.6(10)^{-8}$	$4.6(10)^{-9}$
Na	$2.3(10)^{-10}$	$2.3(10)^{-11}$	$2.3(10)^{-11}$	$2.3(10)^{-12}$
MBBA	$7.8(10)^{-5}$	$7.8(10)^{-6}$	$7.8(10)^{-6}$	$7.8(10)^{-7}$
GaAs	$1.5(10)^{-4}$	$1.5(10)^{-5}$	$1.5(10)^{-5}$	$1.5(10)^{-6}$

Using the above data the values for $J(dP \times t_{rt})$ were calculated for L=2, .2 and α=1, .1. These numbers represent the minimum energy for a switching event that appears as a loss. The values for J are tabulated below.

J (Joules)

	α=1 L=2	α=1 L=.2	α=.1 L=2	α=.1 L=.2
Ruby	$7.6(10)^{-21}$	$7.6(10)^{-22}$	$7.6(10)^{-23}$	$7.6(10)^{-24}$
Na	$1.8(10)^{-21}$	$1.8(10)^{-22}$	$1.8(10)^{-23}$	$1.8(10)^{-24}$
MBBA	$5.1(10)^{-18}$	$5.1(10)^{-19}$	$5.1(10)^{-20}$	$5.1(10)^{-21}$
GaAs	$1.5(10)^{-24}$	$1.5(10)^{-25}$	$1.5(10)^{-26}$	$1.5(10)^{-27}$

The value of log J vs. log t for α=1, L=2 is plotted in Figure 11.

Materials are thus postulated that have nonlinear effects which are real, but have losses at the theoretical limit. None of the bistable systems considered here could function at the limiting speed nor could they show the ultimate loss. However, they serve to point out that the switching energy is not the same as the energy loss at the switch. Thus, the switching energy is provided by an external source, and the production of heat, which limits device density, can be projected to be extremely low.

General thermodynamic arguments may be made that because the entropy is changed by switching, a minimum energy of kTln2 must be involved (Reference 17). In this case the kT energy factor refers to the minimum energy required for switching and is not a minimum energy dissipation. The switching energy for a bistable device is provided by the input optical beam, and it is this energy that the kT factor refers to.

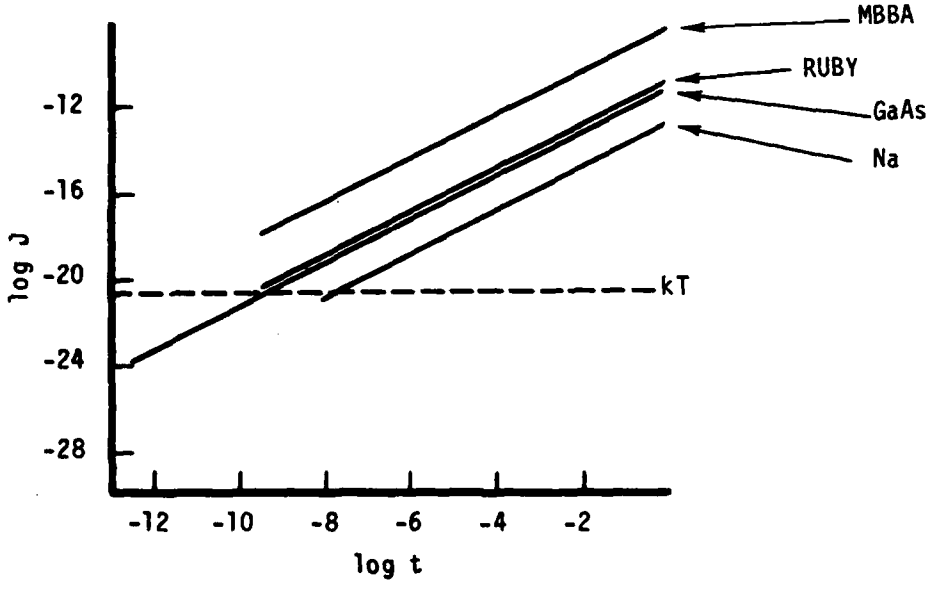

Figure 11. Log J vs. Log t for α=1, L=2

REFERENCES

1. A. Szoke et al., Appl. Phys. Lett. 15, 376 (1969).
2. H. Gibbs et al., Phys. Rev. Lett. 36, 1135 (1976).
3. T. Bischofberger and Y. Shen, Appl. Phys. Lett. 32, 156 (1978).
4. P. Smith and E. Tuner, Appl. Phys. Lett. 30, 280 (1977).
5. E. Garmire et al., Appl. Phys. Lett. 32, 370 (1978).
6. P. Cross et al., IEEE J. Quantum Electron, QE-14, 577 (1978).
7. P. Smith et al., Appl. Phys. Lett. 33, 24 (1978).
8. Y. Lu, "Catastrophe Theory," Springer-Verlag (1976).
9. T. Venhatesan, Appl. Phys. Lett. 30, 282 (1977).
10. A. Huang et al., Appl. Opt. 18, 149 (1979).
11. G. Birkhoff and S. MacLane, "A Survey of Modern Algebra," 4th ed., McMillan, New York (1977).
12. N. Szabo and R. Tanaka, "Residue Arithmetic and Its Applications To Computer Technology," McGraw-Hill (1967).
13. R. Keyes, Proc. IEEE 63, 740 (1975).
14. R. Keyes and J. Armstrong, Appl. Opt. 8, 2549 (1969).
15. W. Kaiser and M. Maier in Laser Handbook Vol. 2, North Holland 1972.
16. T. Miyashita et al., IEEE/OSA Topical Meeting on Fiber Communications, Washington, DC 1979.
17. R. Landauer, IBM Journal, 183, July 1961.
18. H. Gibbs et al., IEEE/OSA Conference on Laser Engineering and Applications, Washington, DC, May 1979; H. Gibbs et al., Optics News, Summer 1979.